Solvent and Intramolecular Effects on the Absorption Spectrum of Betaine-30

John Lobaugh and Peter J. Rossky*

Institute for Theoretical Chemistry, Department of Chemistry and Biochemistry, University of Texas at Austin, Austin, Texas 78712

Received: September 24, 1999; In Final Form: November 10, 1999

The effect of solvent electrostatics and solute torsional modes on the absorption spectrum of betaine-30 in acetonitrile is examined. Combined quantum/classical molecular dynamics ground state simulations are used to calculate the electronic absorption spectrum in acetonitrile. The model for betaine-30 includes the electronic degrees of freedom of the π system of the molecule and their interactions with the electric field of the solvent, treating the electronic wave function at the level of Pariser−Parr−Pople semiempirical electronic structure theory. The absorption intensity, width, and maximum of the S_0 to S_1 band are well reproduced by the model. In solution, the S_0 molecular dipole moment is found to be strongly enhanced due to solvent-induced electronic reorganization. The width of the absorption band in acetonitrile is found to be a function of solvent orientational fluctuations and is not correlated with conformational changes caused by torsional motion in the molecule. This fact, combined with the good agreement between the classical reorganization energies inferred from the simulated and experimental spectra indicates that, at least in acetonitrile, the classical component of the reorganization energy is fully determined by solvent orientational polarization. The spectral band maximum of the lowest energy transition is found to be blue shifted over 7000 cm^{-1}, compared to a calculation in which the coupling of the betaine-30 electronic structure to the solvent molecules is eliminated, in agreement with the shift found experimentally for betaine-30 in acetonitrile compared to alkanes. However, in contrast to the result found in acetonitrile, the transition energy in the absence of solvent interactions is found to be strongly correlated with the central phenolate−pyridinium dihedral ring angle. This contrasting behavior implies that in nonpolar solvents, the classical reorganization energy does have a contribution from that torsional mode. Correspondingly, this difference in behavior with solvent indicates that the assumption of a solvent independent intramolecular contribution to the reorganization energy is questionable.

1. Introduction

The influence of solvent on the electronic absorption spectrum of a molecule can result in changes in peak position, line shape, and intensity, an effect that has been termed "solvatochromism".[1] Correspondingly, the solvatochromic shifts that arise in different solvents can serve as a useful empirical measure of solvent polarity. A number of scales exist,[2] one of the more popular being the $E_T(30)$ scale. The $E_T(30)$ scale makes use of the lowest energy transition of the *N*-pyridinium-phenolate, betaine-30. The $E_T(30)$ values, which are simply the energies of the absorption maxima in kcal/mol, have been measured for over 200 solvents.[3] The S_0 to S_1 transition in betaine-30 is particularly well suited for use as a measure of solvent polarity. The band, which is a π to π^* transition, is well separated from the other electronic transitions making its identification and maximum unambiguous. Further, it is enormously sensitive to solvent polarity shifting over 10 000 cm^{-1} from 11 470 cm^{-1} in diphenyl ether to 22 080 cm^{-1} in water.[2] The transition corresponds to an intramolecular electron transfer from the phenolate ring of the molecule to the pyridinium ring as shown schematically in Figure 1. The extreme sensitivity of the solvatochromic shift is due to the large dipole moment change between ground and lowest excited state. The band is blue shifted as a function of increasing polarity due to the much larger dipole moment in the ground state. In fact, betaine-30 is a member of a large group of compounds where the degree and direction of the solvatochromic shift depends on whether the charge separated zwitterionic state is predominate in the ground or the excited state.[2] For later consideration, we note a number of distinct characteristics of the spectrum of betaine-30. Not only is the peak position of the band sensitive to the nature of the solvent, but also its shape and width. The band shape is markedly asymmetric, having increased absorption on the high-frequency side.[4] The degree of solvent broadening increases as

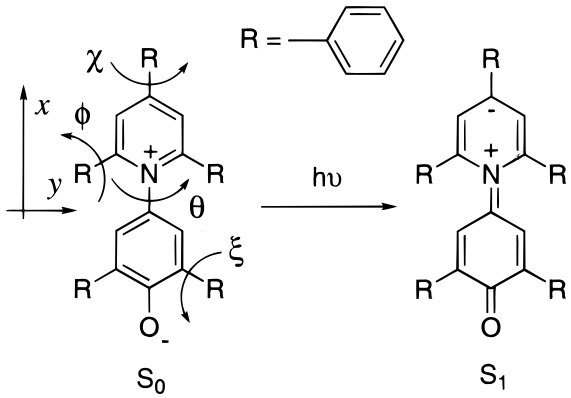

Figure 1. Schematic of the ground to first excited state electronic transition in betaine-30. The reference frame for calculating the Cartesian components of the transition and permanent dipoles is as follows: the *x* axis is along the principal axis of the molecule, the *y* axis is perpendicular to the *x* axis and is confined to the plane of the pyridinium ring, and the *z* axis is perpendicular to the plane of the pyridinium ring.

10.1021/jp993444u CCC: $19.00
Published on Web 02/03/2000

a function of solvent polarity,[4,5] although at low solvent polarities the absorption width is largely independent of solvent type. A band shape analysis for betaine-30[5] and the related compound betaine-26[4] in the context of electron transfer (ET) formalism[6−8] links this increasing broadening with solvent polarity to the increasing solvent reorganization energy associated with electron transfer. According to the analysis, the asymmetry results from the vibronic substructure of the electronic transition. In the case of polar and nonpolar aprotic solvents, the band is well fit with a single effective molecular mode of approximately 1600 cm^{-1}, taken to be indicative of a vibrational mode within the molecule involving C−C, C−N, or C−O character.[4]

Empirical scales, such as the $E_T(30)$ scale, and continuum-based theories, such as the ET theory cited above, lack information about the precise molecular interactions that give rise to the solvatochromic shift and broadening and therefore provide motivation for a theoretical molecular-based model to analyze these effects. One approach is an integral equation formulation recently applied for a simplified molecular solvent to analyzing the $E_T(30)$ scale in terms of component solvation forces.[9] Alternatively, a molecular dynamics (MD) simulation approach can be taken, using empirical solvent solute potentials. Such an approach to the solvatochromism has been taken very recently by Maroncelli and co-workers in a study of betaine-30 in a wide range of solvents.[10] To provide a more complete description of the absorption band, including line shape, MD simulation combined with a suitable electronic structure formalism can be used to provide a deeper analysis.[11] Such an approach is taken here, using combined classical/quantum MD simulations of betaine-30 in a polar solvent, acetonitrile. An atomistic model of the betaine-30 is used with the inclusion of an appropriate subset of both the electronic and solute nuclear degrees of freedom in the MD simulation. This is done in order to capture the critical effects due to the solvent, as well as conformational changes of the betaine-30. The goal is to ascertain the detailed roles of the solvent and intramolecular degrees of freedom in establishing the spectral behavior.

In section 2, we present the methods used in the calculation, including electronic structure, simulation, and spectral elements. Section 3 describes the results, including an analysis of the molecular contributions to spectral line shapes. The conclusions are presented in section 4. An appendix providing further details of the algorithm development is provided in the form of Supporting Information.

2. Methods

Potential Energy Functions. The approach here is different from conventional MD simulations where molecular interactions are modeled solely through the use of effective potential energy functions. Direct inclusion of the key electronic degrees of freedom of the solute necessitates the recalculation of the solute wave function at every MD time step. This task can be computationally very demanding, even for relatively small molecular systems. Nevertheless, so-called ab initio MD[12,13] has been applied to relatively large systems for relatively short time simulations. Here, an alternative approach is taken: we limit the electronic degrees of freedom to the π system of the betaine-30 solute. The three lowest energy bands in the UV/visible solution spectrum of betaine-30 are π to π^* transitions,[14] and accordingly only the electrons of the π subsystem are critical to the present model. The σ electrons, lone pair electrons, inner shell electrons and nuclei are combined and treated as classical effective nuclear cores. Each nuclear core has a formal integer positive charge equal to the number of 2p electrons it donates to the π system. A semiempirical electronic structure method is used to treat the π electrons that interact with themselves and with the nuclear cores of the betaine-30 and solvent molecules. The electronic structure method used here is the Pariser−Parr−Pople (PPP) method.[15−17] The method has proved to be quite accurate in reproducing ground state properties as well as transition energies of aromatic and conjugated systems.[18] There are, of course, several methods which make use of combined quantum mechanical and classical molecular empirical potentials. In particular, we note at the outset that our approach is very similar to the pioneering QCFF/PI method,[19,20] although it differs in detail. All valence electron treatments, such as the QM/MM method of Field et al.,[21] incorporate the same elements.

In addition to the electron−core, electron−solvent, and electron−electron interactions, there are several other interactions that must be specified in order to complete the model. The remaining interactions are the nuclear core interactions with themselves and with the solvent molecules as well as the solvent−solvent interactions. These interactions are treated using conventional molecular mechanics interaction terms. Including all the interactions that must be part of the model, the total potential, V_{TOT}, is written

$$V_{TOT} = V_\pi + V_{C-C} + V_{S-S} + V_{C-S} \tag{1}$$

where V_π is the electronic part of the potential, which includes the electron−electron, electron−core, and electron−solvent interactions. The terms V_{C-C}, V_{S-S}, and V_{C-S} denote the core−core interactions of the betaine-30, the solvent−solvent, and core−solvent interactions, respectively. The electronic energy portion of the potential is written as[22]

$$V_\pi = {}^1/_2 \sum_{\mu\nu} P_{\mu\nu}(H_{\mu\nu} + F_{\mu\nu}) \tag{2}$$

where the summation is over the atomic sites that contribute to the π system. The terms $P_{\mu\nu}$, $F_{\mu\nu}$, and $H_{\mu\nu}$ are the bond-order matrix, Fock, and one-electron core matrix elements, respectively. The bond-order matrix elements are given by

$$P_{\mu\nu} = 2\sum_i^n c_\mu^i \, c_\nu^i \tag{3}$$

where the product of molecular orbital coefficients c_μ^i and c_ν^i at sites μ and ν is summed over occupied molecular orbitals (in this case $n = 22$). The Fock matrix elements are given in the PPP method by[18]

$$\begin{aligned} F_{\mu\nu} &= H_{\mu\nu} - {}^1/_2 P_{\mu\nu}\gamma_{\mu\nu} \quad (\mu \neq \nu) \\ F_{\mu\mu} &= H_{\mu\mu} + {}^1/_2 P_{\mu\mu}\gamma_{\mu\mu} + \sum_{\rho \neq \mu} P_{\rho\rho}\gamma_{\mu\rho} \end{aligned} \tag{4}$$

where $\gamma_{\mu\nu}$ are the two-electron repulsion matrix elements.

The parameterizations and functional forms for the PPP matrix elements are, of course, not uniquely defined. The particular functional form and parameterization that are given below are those that have been successful in reproducing transition energies and intensities in aromatic heterocycles.[23] An approximate form for the two-electron repulsion integral $\gamma_{\mu\nu}$ that has been particularly successful in reproducing molecular spectra in general[18] is the Mataga−Nishimoto relationship,[24] given by

$$\gamma_{\mu\nu} = \frac{e^2}{(R_{\mu\nu} + a_{\mu\nu})}$$

$$a_{\mu\nu} = \frac{2e^2}{(\gamma_{\mu\mu} + \gamma_{\nu\nu})} \quad (5)$$

where e is the magnitude of the electron charge, $R_{\mu\nu}$ is the distance between atoms μ and ν, and $\gamma_{\nu\nu}$ is the one-center repulsion parameter. The values for the γ parameters used here, based on the analysis of Hinze and Jaffé,[18,25] are listed in Table 1. The off-diagonal elements, $H_{\mu\nu}$, of the one-electron core matrix are treated at the same level of approximation as Hückel theory, in that a nearest neighbor approximation is used. That is,

$$H_{\mu\nu} = \beta_{\mu\nu} \quad \mu, \nu \text{ covalently bonded}$$

$$H_{\mu\nu} = 0 \quad \text{otherwise } (\mu \neq \nu) \quad (6)$$

Once again, a number of alternative approximations have been used in the PPP method for the resonance parameter β.[18] The Linderberg approximation,[26] notable for the fact that it can be calculated a priori, has been used successfully in the calculation of the spectra of heteronuclear aromatic systems as stated above[23] and is given by

$$\beta_{\mu\nu} = (\hbar^2/m_e) R_{\mu\nu}^{-1} \frac{dS_{\mu\nu}}{dR_{\mu\nu}} \quad (7)$$

where $\hbar$ is Planck's constant over 2π, m_e is the electron mass, and $S_{\mu\nu}$ is the overlap integral between atomic orbitals μ and ν. Slater orbitals with exponents determined from the usual screening rules[27] were used to determine the gradient term in eq 7. The resulting values are listed in Table 1. The diagonal elements, $H^0_{\mu\mu}$, of the one-electron core matrix are approximated in the PPP method as

$$H^0_{\mu\mu} = \alpha_\mu - \sum_{\rho \neq \mu} Z_\rho \gamma_{\mu\rho} \quad (8)$$

The first term of eq 8 is the energy of the orbital μ in vacuo in its appropriate valence state. While α is not strictly a spectroscopic value, the valence state ionization data of Hinze and Jaffé[25] has been the most popular[18] and the corresponding atomic values are included in Table 1. The second term is the interaction of the electron at site μ with the nuclear core at site ρ, which has formal charge Z_ρ (equal to the number of 2p electrons the atom donates to the π system). The functional form of the interaction is made the same as the two-electron repulsion term for consistency.

Having specified the electron−electron interactions and core−electron interactions in the PPP Hamiltonian, it still remains to specify the important element that describes how the solvent interacts with the π electron system. The PPP method is modified here to include the solvent−electron interactions by adding a third term to eq 8

$$H_{\mu\mu} = H^0_{\mu\mu} - \sum_j \frac{eq_j}{R_{j\mu}} \quad (9)$$

The additional term is the matrix element due to the electron−solvent charge interaction where the electron is in the atomic orbital centered at μ and $R_{j\mu}$ is the distance between the nuclear core μ and the jth solvent site with partial charge q_j. The inclusion of a distance cutoff for interactions in the MD simulation is accomplished by multiplying the solvent−electron Coulomb terms in eq 9 by a suitable cutoff function. In the present calculation, we neglect potential contributions to the solute−solvent interactions associated with differences in polarizability and dispersion interactions between the ground and excited states.

TABLE 1: PPP Parameters and Bond Lengths

site	α_μ (eV)	$\beta_{C\mu}$ (eV)	$\gamma_{\mu\mu}$ (eV)	C−X bond length (Å)
C	−11.17	−2.2595	11.13	1.395
N	−25.73	−2.0166	16.76	1.395
O	−17.70	−2.6000	15.23	1.23
H				1.08

TABLE 2: Nonbonded Interaction Parameters for Betaine-30 (eq 1)

atom pair	A[a]	α (Å^{-1})	B (kcal/mol Å^6)
HH	0.659×10^4	4.082	0.492×10^2
CH	4.474×10^4	2.041	1.2496×10^2
CC	2.994×10^5		3.253×10^2

[a] Units for HH are kcal/mol, CH are kcal/mol Å^6, and CC are kcal/mol Å^{12}.

The core−core interaction V_{C-C} is made up of two terms:

$$V_{C-C} = \sum_{\mu\nu} \gamma_{\mu\nu} Z_\mu Z_\nu + V_{nb} \quad (10)$$

The first term is the core−core repulsion, which is typically estimated using a Coulombic model with an integer charge of Z_μ at each nuclear site μ. However, as pointed by Chung and Dewar,[28] this is inconsistent with the functional form assigned previously to the electron−electron and core−electron interactions. Accordingly, the interaction is written as above using the same form as $\gamma_{\mu\nu}$ for the two-electron repulsion matrix element. The second term accounts for the steric effects within the molecule that arise from the so-called nonbonded interactions. These interactions have been found to be critical in correctly estimating barriers to torsional motion in systems modeled using the PPP method.[18] The empirical functions of Bartell[29] have been found to be adequate to reproduce the gas phase conformation of diphenyl;[30] they are used here without further modification. They are:

$$V_{HH} = A_{HH} \exp(-\alpha_{HH} r) - B_{HH} r^{-6}$$

$$V_{CH} = A_{CH} r^{-6} \exp(-\alpha_{CH} r) - B_{CH} r^{-6} \quad (11)$$

$$V_{CC} = A_{CC} r^{-12} - B_{CC} r^{-6}$$

where r is the distance between two nonbonded atoms in the betaine-30 molecule. The parameters used in the above equations are listed in Table 2. In the present model, the interactions are needed only between nonbonded pairs of atoms for which relative motion can occur as a result of ring torsion (see below).

Torsional motion of the rings modifies the π electronic energy due to the variation in conjugation across the bonds' connecting rings. This has been accounted for by assuming that the resonance integral between the sites μ and ν that connect two rings has the following parametric form as a function of the torsional angle θ:

$$\beta_{\mu\nu} = \beta^0_{\mu\nu} \cos\theta \quad (12)$$

where $\beta^0_{\mu\nu}$ is the resonance integral for the planar system. Apart from rigid ring rotations around the six dihedral angles

TABLE 3: Lennard-Jones Parameters for Betaine-30

site	σ (Å)	ϵ (kcal/mol)
O[a]	2.96	0.21
N[b]	3.25	0.17
C[c]	3.55	0.07
H[c]	2.42	0.03

[a] Values are taken from the OPLS potential function parameters for O in R−C═OR groups.[54] [b] Values are taken from the OPLS potential function parameters for N in pyridine.[54] [c] Values are taken from an all-atom model of benzene.[55]

identified in Figure 1, all other internal degrees of freedom in betaine-30 were frozen through the use of constraint dynamics in the simulations. This constraint can be viewed as resulting from an adiabatic separation of intramolecular vibrations from the ring torsional motion and solvent fluctuations. As long as the high frequency vibrational modes are weakly solvent configuration dependent, the vibronic substructure from these modes is an effect that could be added a posteriori to the simulation results presented in this paper. Since the primary goal of the present study is to examine the effect of solvent and conformation on the absorption spectrum, the inclusion of higher frequency vibrational modes in the potential is not pursued here. The various fixed bond lengths of the molecular geometry used are given in Table 1.

The solvent−solvent interactions (V_{S-S}) were modeled with the rigid three site model for acetonitrile of Edwards, Madden, and McDonald.[31] The solvent intermolecular potential consists of Coulombic and Lennard-Jones functions with the interaction sites at the atomic positions of the methyl carbon, carbon, and nitrogen. The core−solvent interaction, V_{C-S}, consists of two terms: The first term comprises the Coulombic interactions

$$V_{C-S} = \sum_{j\mu} \frac{Z_\mu q_j}{R_{j\mu}} + 4\epsilon_{j\mu}\left(\left(\frac{\sigma_{j\mu}}{R_{j\mu}}\right)^{12} - \left(\frac{\sigma_{j\mu}}{R_{j\mu}}\right)^{6}\right) \qquad (13)$$

between the partial charges of the solvent and the charged cores of the betaine-30 molecule. The second term includes Lennard-Jones (LJ) interactions between all the betaine-30 atoms (including the hydrogens) and solvent sites. The LJ parameters used for betaine-30 are listed in Table 3. The solvent LJ parameters and partial charges were the same as those used for the solvent−solvent potential. The usual Lorentz−Berthelot mixing rules[32] were used to calculate the appropriate Lennard-Jones interaction parameters $\epsilon_{j\mu}$ and $\sigma_{j\mu}$ between the betaine-30 atoms and solvent sites.

We note that, in the present work, we do not treat solvent electronic polarizability explicitly. However, the effective pair potential model for the solvent exhibits an enhanced polarity (dipole and higher moments) compared to the gas-phase molecule, accounting for the average polarization of each molecule by the liquid environment. It has been argued that the inclusion of explicit solvent polarizability and of the difference in solute polarizability between the ground and excited states are important factors in the correct evaluation of spectral shifts.[33] The latter factor would result in a difference in dispersion forces for the two electronic states, with the excited state expected to be more strongly interacting with the solvent. For a quantitative reproduction of experimental spectral positions, these effects are no doubt significant, particularly for solvents lacking a permanent dipole moment. However, it is important to note that the quantitative error associated with the use of effective pair potential models[34] is not yet established. Calculations that do not account explicitly for polarizability effects have successfully reproduced experimental results in many cases,[10,34−36] while other reports suggest that these effects are critical.[33] In the most detailed fully molecular study available,[37] the effect of explicit solvent polarizability on spectral position and line shape was found to be quite small, as long as the total (electronic plus orientational) polarizability of the solvent molecular models were the same. Hence, it is clear that further research aimed at developing accurate schemes for treating explicit polarizability effects on spectra is desirable.

Here, our goal is not to predict the solvatochromic shift per se. Rather, for a simulation that reasonably reproduces the measured shift and line shape, we wish to dissect the elements contributing to these characteristics. Considering this goal and the discussion above, we believe that a model lacking explicit treatment of polarizability is completely sufficient for the present purposes, and we proceed on that basis.

Simulation Details. With the exception of the electronic potential V_π (see eq 2), all of the terms in the total potential are simple analytic functions of the nuclear coordinates. On the other hand, derivatives of elements of the bond-order matrix in eq 2 are problematic given the lack of analytic expressions for the coordinate dependence of the molecular orbital coefficients. However, for the same reason that analytic derivative methods in conventional quantum chemistry are efficient, evaluation of the forces for the propagation of MD trajectories can also be readily carried out. This is because the molecular orbital coefficients are found by variational minimization of the total electronic energy to give the resulting ground state SCF energy that is V_π. Correspondingly, the derivatives of the bond order matrix elements in eq 3 do not appear in evaluation of the derivative of eq 2 with respect to a nuclear coordinate[22,38] (an explicit proof for the ground state energy is given in ref 39).

The equations of motion were integrated using the velocity Verlet algorithm[32] and a time step of 10 fs. The simulations were run at 298 K at a solvent density of 0.7867 g/cm^3. A total of 1200 acetonitrile molecules were used to determine the size of the simulation box. After the solvent was equilibrated the betaine-30 molecule was inserted into the simulation box. Any solvent molecule that had overlapping LJ radii with the betaine-30 was removed from the simulation cell. A total of 1172 solvent molecules were retained for simulation with the betaine-30, and then the system was equilibrated. The simulation was run with the Nosé equilibration technique.[40−42] All Coulombic interactions were truncated with a smooth cutoff of half the box length.[43]

As stated previously, constraint dynamics were used to maintain the rigidity of the acetonitrile and the betaine-30. A conventional method for maintaining constraints in the velocity Verlet algorithm has been the RATTLE method.[44] However, due to their reduced dimensionality, both linear triatomics and molecules containing planar rings are problematic for iterative constraint methods such as RATTLE and SHAKE as they were originally outlined.[44,45] To circumvent this problem the constraint method of Cicotti, Ferrario, and Ryckaert was used[46] for the propagation of the equations of motion. The method as described in ref 46 is for the Verlet integrator and uses an iterative constraint algorithm similar to SHAKE for the numerical implementation of constraint dynamics. The method can be modified for the velocity Verlet integrator using an algorithm similar to RATTLE. Details for this generalized RATTLE-type method have recently appeared[47] and will not be repeated here. A single Nosé−Hoover oscillator was attached to the Cartesian degrees of freedom of the acetonitrile molecules. The use of a Nosé−Hoover oscillator requires that the velocity Verlet

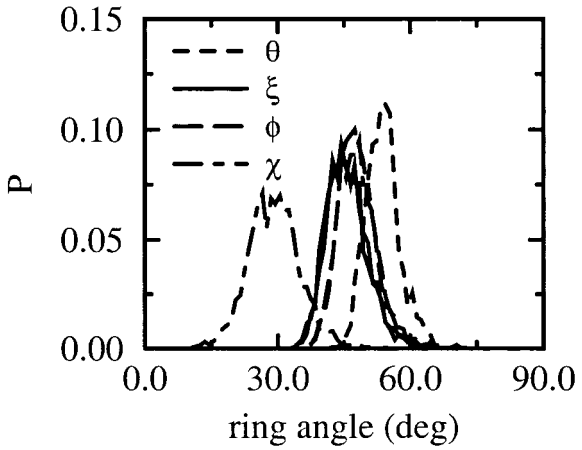

Figure 2. Distribution of ring angles of betaine-30 in solution for the B conformation of pendant rings (see text). Notation for each ring angle is given in Figure 1.

algorithm be modified to account for the coupling of the Nosé−Hoover oscillator to the solvent particle velocities. The implicit iterative algorithm of Tuckerman et al.[48] was used for the velocity Verlet integrator. The algorithm must be modified due to the fact that holonomic constraints were used to maintain the rigidity of the acetonitrile molecules. Details of how the velocity Verlet integrator algorithm was coupled to the constraint method are given in an appendix, provided as Supporting Information.

Transition Energies and Intensities. Solute excited states were calculated using configuration interaction with single excitations. Spectra were calculated with all possible single excitations. Transition energies calculated at this level of theory have been shown to be adequate to reproduce experimental absorption spectra values for a large variety of conjugated heterocycles.[23] Intensities were calculated using the dipole length expression and assuming zero-differential overlap (ZDO) between atomic orbitals.

3. Results and Discussion

Molecular Conformation. Previously published electronic structure calculations using the AM1 model Hamiltonian on betaine-30[49] have found two minimum energy conformations (which are referred to hereafter as A and B) that differ energetically by 0.1 kcal/mol in the gas phase and an estimated 1 kcal/mol in solution. The conformations differ by rotation of one of the phenyl rings attached to the phenolate by an angle of 2ξ (see Figure 1) through the plane of the phenolate ring (see also Figures 2 and 3 in ref 49). Both conformations were also identified in this calculation, with gas phase energies within 0.5 kcal/mol using the present PPP description. The ring angles of both gas phase conformations were also in good agreement (within 7°) with those found from the AM1 Hamiltonian.[49] Here, each conformation was used as an initial starting point for a separate 100 ps MD run. In both cases, the conformation of the molecules fluctuated locally around their initial gas phase minimum energy conformations over the course of the MD trajectory in solution and did not interconvert. The distribution of angles sampled by the molecule for conformation B is shown in Figure 2. The angle distributions and lack of interconversion indicate that rotational well depths are considerably larger than thermal energies. The most probable values for the present angular distributions are in good agreement with the reported values for the minimum energy conformation calculated using the AM1 Hamiltonian using a dielectric continuum[49] model for the solvent.

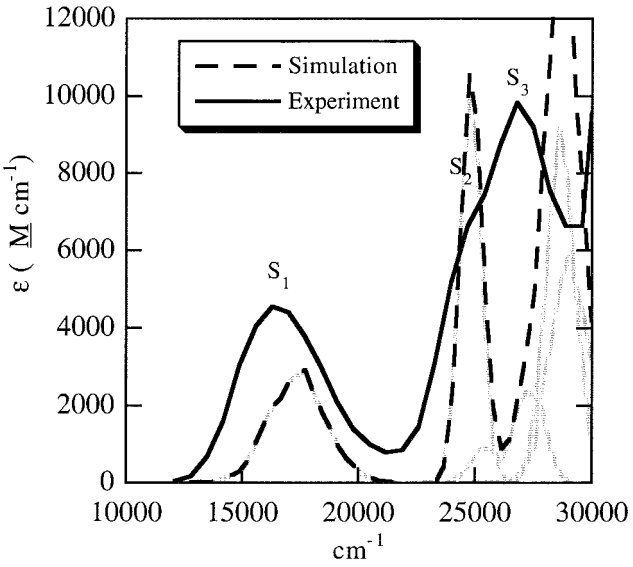

Figure 3. Simulated (dashed line) and experimental[3] (solid line) electronic absorption spectrum of betaine-30 in acetonitrile. The individual transitions in the simulated spectrum are shown as gray lines.

It is important to note that the central angle between the pyridinium and phenolate rings (θ in Figure 1) takes on a strongly nonplanar value, as is evident in Figure 2. This important result is not noted in some earlier work[49] but has been noted by others.[50] The twist from planar is a result of significant steric interactions between the pendant phenyl groups. The presence of a comparable ground state twist using the AM1 Hamiltonian has been verified by our own calculations, so that this is not a figment of the model used here. A very recent report from the Maroncelli lab[10] has also identified such a distortion, with a twist angle for the minimum energy conformer of 48°, close to the present average value of 53°.

Moments and Absorption Spectrum. The calculated spectra for conformations A and B were found to be statistically indistinguishable. The calculated spectrum for conformation B, accumulated over the 100 ps run, is shown in Figure 3. The result is displayed as the extinction coefficient, derived directly from transition dipole matrix elements.[51] The spectral calculation included the five lowest energies; the total spectrum in Figure 3 is shown as a dashed line while the gray lines indicate the individual calculated subbands for each transition. The calculated intensity and absorption maximum of the lowest energy transition is in reasonably good agreement with the experimental peak, as can be seen from the experimental spectrum which has also been included in Figure 3. The simulated $S_0 \rightarrow S_1$ maximum yields an $E_T(30)$ value of 50.6, while experimentally[2] one finds an $E_T(30)$ value of 46.0.

The Cartesian components of the transition dipoles were averaged over the trajectory using the internal reference frame shown in Figure 1. The permanent dipole moments of the ground state and three lowest energy excited states were also calculated using the ZDO approximation and Mulliken charge estimates at the atomic sites of the betaine-30. The average dipole moments and their components are listed in Table 4. The average transition dipole from the ground to the first excited state is oriented along the principal axis of the molecule with very small components along the remaining two axes, indicating that the first excited state is a charge transfer state. The concomitant reduction of the permanent dipole moment of the first excited state confirms a characterization of the transition as a charge transfer from the phenolate to the pyridinium ring.

The energies of the second and third peaks are also

TABLE 4: Permanent and Transition Dipole Moments for Betaine-30[a]

state	permanent	transition dipole moment components (D)		
	$\|\vec{\mu}\|(\|\mu_x\|)$ (D)	$\|\mu_x\|$	$\|\mu_y\|$	$\|\mu_z\|$
	A. Calculated Average Values in Acetonitrile Solution			
S_0	24.95 (24.94)			
S_1	5.5 (2.49)	2.1	0.04	0.04
S_2	20.7 (20.04)	0.06	1.0	1.7
S_3	10.2 (8.55)	0.2	0.9	0.3
	B. Calculated Average Values without Solute−Solvent Interactions			
S_0	15.8 (15.8)			
S_1	7.4 (4.2)	4.1	0.06	0.03
S_2	8.0 (6.9)	0.08	0.7	0.03
S_3	9.8 (8.7)	0.04	0.2	0.3

[a] The internal reference frame used to calculate the Cartesian components of the transition and permanent dipole moments is defined in Figure 1.

comparable to those in the observed solution spectra, although the intensity of the calculated S_2 transition (just below 25 000 cm^{-1}) is clearly far too large too contribute only a shoulder, while that for S_3 (at about 26 000 cm^{-1}) is correspondingly too small. The solution spectrum is evidently congested with multiple overlapping states at higher energy, so comparison is not productive. Analysis shows that the transition dipole for the calculated second excited state has only a very small component along the principal axis and a large dipole comparable to that of the ground state, indicating that it is a localized excitation rather than one characterized as charge transfer. The third excited state S_3 found here corresponds to a charge transfer excitation (although weaker than that to S_1, as is evident from the subband intensity), judging from the reduction of the permanent dipole moment compared to the lowest energy state and an appreciable transition dipole moment component along the principal axis. The results calculated for the second and third excited states and their characterization as localized and charge transfer states, respectively, are not in agreement with the analysis of the solvent dependence of the static absorption spectrum by Barbara and co-workers.[14] Experimentally, variation of transition energy with solvent polarity shows that the shoulder in Figure 3 at about 25 000 cm^{-1} is a charge transfer excitation to S_2, while the more intense peak at about 27 000 cm^{-1} is apparently a weak localized excitation to S_3. Thus, the relative energy of the closely spaced second and third excited states (calculated to lie at 25 000−26 000 cm^{-1}) is evidently reversed in the present calculations. We attribute this difficulty to the limitations of the very simplified single CI model used here in describing the higher excited states accurately, although the primary excitation to S_1 appears to be described well.

Before proceeding, it is worth noting that the gas phase permanent dipole moment values computed for the S_0 state are comparable to those obtained with semiempirical quantum chemistry[49,50] and are also close to the value inferred experimentally in relatively nonpolar solvent.[2] However, it is important to note the very large enhancement in the dipole moment that we find in acetonitrile solution (see Table 4). This enhancement effect is also seen in a dielectric continuum solvent description using AM1,[49] although the effect is somewhat smaller, and a comparable increase has been noted in earlier semiempirical CI calculations.[50] Inclusion of such enhancement seems likely to be important in the modeling of solutions when the electronic structure is not treated explicitly. In any case, the use of the experimentally quoted or gas phase value in such models[34,10] adds an additional uncertainty to the comparison of models and experiment.

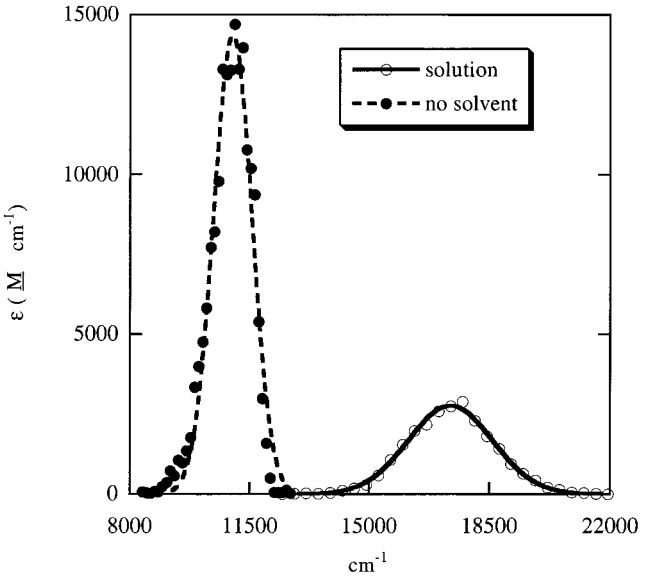

Figure 4. S_0 to S_1 electronic transition calculated in acetonitrile (open circles) and without solvent interactions (filled circles). The lines are Gaussian fits to the simulation data using eq 14 for acetonitrile (solid line) and without solvent (short dashed line). The reorganization energies calculated from the simulated data are 3625 cm^{-1} in acetonitrile and 763 cm^{-1} in the absence of solvent interactions.

The electronic transitions are inhomogeneously broadened by the fluctuations in the transition energy and intensities over the MD trajectory. The evident inhomogeneous broadening has two possible sources. First, broadening may be due to the distribution of solvent configurations that are sampled. The resulting fluctuations in the solvent reaction field would then give rise to a band. Broadening may also be due to fluctuations in the intramolecular degrees of freedom of the betaine-30, which, in the case of this study, are the torsional motions of the rings of the molecule. We now consider the important issue of the relative contribution of each source in detail, for the transition to S_1. Multiphonon band theory[6−8] has been used to analyze the solvent bandwidth dependence and asymmetry features of the charge transfer transition of betaine-26[4] and betaine-30.[5] The line shape theory in the form applied to betaine-26 and betaine-30 models the line shape as a set of Gaussians in a vibronic manifold. The Gaussian profile arises from the continuous dispersive media and the vibronic substructure from effective discrete local modes. Since the simulation carried out here does not include skeletal intramolecular vibrations of the solvent or betaine-30, the line shape should be well fit by a single Gaussian and, as can be seen from Figure 3, it does not exhibit the pronounced asymmetry on the high frequency side that results from such vibrational transitions. The form of the line shape function as a function of frequency ν, in the absence of discrete quantum modes, is given by

$$K(\nu) = \sqrt{\frac{\pi k_B T}{\lambda_{cl}}} \exp\left(-\frac{(h\nu - \lambda_{cl} + \Delta G_0)^2}{4k_B T \lambda_{cl}}\right) \qquad (14)$$

where λ_{cl} is the classical, typically outersphere, reorganization energy, ΔG_0 is the overall free energy of reaction, k_B is Boltzmann's constant, T is the temperature, and h is Planck's constant. A fit of the spectrum to this form yields the two parameters, λ_{cl} and ΔG_0. The fit of eq 14 to the calculated first absorption peak is shown in Figure 4. The inferred solvent reorganization energy is 3625 cm^{-1}, which is in remarkably good agreement with the value of 3644 cm^{-1} calculated from

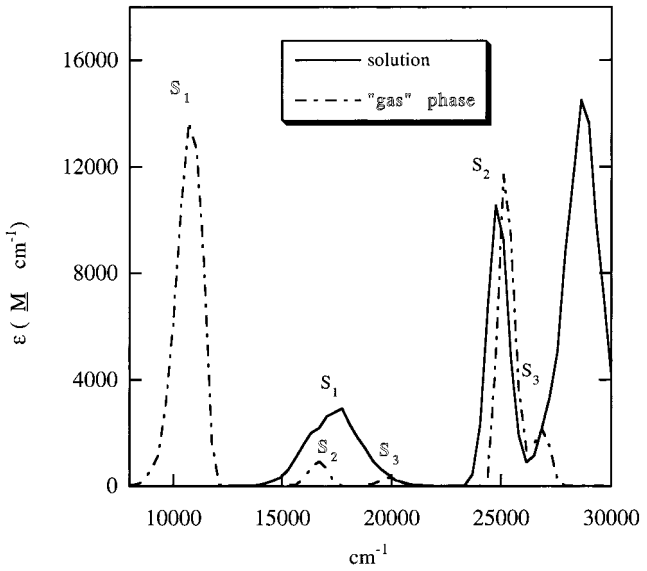

Figure 5. The simulated electronic absorption spectrum in acetonitrile (solid line) and calculated without solvent interactions (dot−dashed line). The locations of the individual transitions are labeled in solid font for the solution spectrum and in outline font for the transitions calculated without solvent interactions.

the fit to the experimental spectrum.[5] This very close agreement is presumably in part fortuitous. The result is also close to the simulated value of 4260 cm^{-1} for a rigid solute, effective potential model.[10] The overall free energy of reaction ΔG_0 is -13753 cm^{-1}, the magnitude of which is similar to, but larger than, that found from the fit to the experimental absorption spectrum ($-11{,}645$ cm^{-1} [5]).

The good agreement with experiment manifest here demonstrates that the model is sufficiently realistic to justify further spectral analysis, which we consider next. To ascertain the relative contribution of intramolecular and solvent broadening to the spectrum, the electronic wave functions and corresponding absorption spectrum were fully recalculated with the same solute configurational set, but *without* including the solvent influence (i.e., $H_{\mu\mu} = H^{(0)}_{\mu\mu}$ in eq 9). The resulting spectrum would be the gas phase spectrum if the gas phase configurational sampling were the same as that for betaine-30 samples in acetonitrile. Alternatively, the spectrum can also be considered to approximate the behavior of the spectrum that would be obtained in a completely nonpolar, nonpolarizable solvent with the plausible corresponding assumption that the distribution of torsional angles shown in Figure 2 is not changed in going from acetonitrile to a nonpolar solvent. As can be seen from Figure 5, the solvent has a profound effect on the wavelength and intensities of the three lowest energy transitions. The S_0 to S_1 transition is shifted over 7000 cm^{-1} from 17 700 cm^{-1} in solution to 10 700 cm^{-1} in the absence of solvent interactions. The value of 10 700 cm^{-1} is in close agreement with the estimated transition energy in long-chain alkane solvents of 10 850 cm^{-1}.[2] The energies of lowest and second (10 700 and 16 700 cm^{-1}, respectively) transitions are also in good agreement with the gas phase INDO/S results of Alencastro et al.[49] which are 11 300 and 16 900 cm^{-1}.

The broadening of the peaks of the "gas" phase or nonpolar solvent spectrum necessarily arises solely due to fluctuations of the conformation of the molecule. To determine which torsional ring angle has the greatest effect on the energy of the S_0 to S_1 transition, the energy gap was plotted at each MD time step as a function of the torsional angles. Not surprisingly, the energy was found to be correlated predominantly with changes in the central ring angle θ (see Figure 1), as shown in Figure 6a. This significant result is also observed in other very recent calculations by Mente and Maroncelli.[10] This indicates that fluctuations in the central ring angle are primarily responsible for the broadening of the peak in the nonpolar solvent or "gas" phase spectrum. In the case of the spectrum calculated using the solvent electrostatic field generated by the acetonitrile molecules, the broadening can arise from ring angle fluctuations and from solvent fluctuations. The corresponding correlation diagram, shown in Figure 6b, generated including the solvent influence (see eq 6), however, reveals that in the polar solvent, the transition energy fluctuations are apparently completely *uncorrelated* with fluctuations in the central ring angle. The fact that this is true is shown in Figure 6c, which gives the angular dependence of the average excitation energy obtained from the data in Figure 6b. The insensitivity evident in Figure 6c is in striking contrast to that manifest in Figure 6a, in the absence of solvent. The results in Figure 6c show clearly that the correlation evident in the gas phase (Figure 6a) is *not* simply hidden by the large solvent fluctuations contributing to the results in solution (Figure 6b). Rather, Figure 6b shows the surprising result that the solvent orientational polarization somehow destroys the dependence of the transition energy on the central ring angle. As a corollary, it follows that in the present calculation, the line shape in acetonitrile is therefore due to solvent fluctuations and not dependent on the distribution of ring angles sampled by the molecule in solution.

There is clear evidence for an electronic effect of the solvent, in that the $S_0 \rightarrow S_1$ transition frequency is highly correlated with the central ring angle in the absence of the polar solvent, but these are essentially uncorrelated in the presence of the solvent field. Analysis of the electronic matrix elements comprising the transition energy reveals that the origin of this surprising result lies in the electronic reorganization of the solute in the presence of the solvent. More specifically, the values of the Coulombic and exchange integrals contributing to the central ring angle dependence are significantly shifted by this electronic reorganization, so that, in the presence of the solvent field, the key matrix elements have relatively small magnitudes and their dependence on the ring angle tend to cancel. In contrast, this is not found to be the case when the solute wave function is evaluated in the absence of the solvent field. While the generality of this behavior is not clear, the result for this solute alone provides an important warning for the interpretation of the solution phase spectra of similar solutes in the general case.

The absorption width is smaller in the gas-phase spectrum, and the resulting fit (see Figure 4) gives a reorganization energy of 763 cm^{-1}. A corresponding value of 1100 cm^{-1} has been estimated by Mente and Maroncelli.[10] Reorganization energies found from fits to the experimental spectra for nonpolar solvents are approximately 1700 cm^{-1} for related molecules and are largely independent of solvent type.[4] The difference between nonpolar solvent reorganization energy from experiment and from the gas phase simulation is consistent with the view[4] that in nonpolar solvents there are additional contributions to the reorganization energy arising from the solvent. At the same time, the present results demonstrate that there are, in general, low frequency solute modes contributing to the "classical" reorganization energy. In the present case, the data in Figure 6a show that the central ring angle is a primary candidate for the dominant solute degree of freedom. However, as shown above, the contribution of this degree of freedom to the classical part of the reorganization energy is evidently *not* simply additive, independent of the solvent. As a result, the separation of this

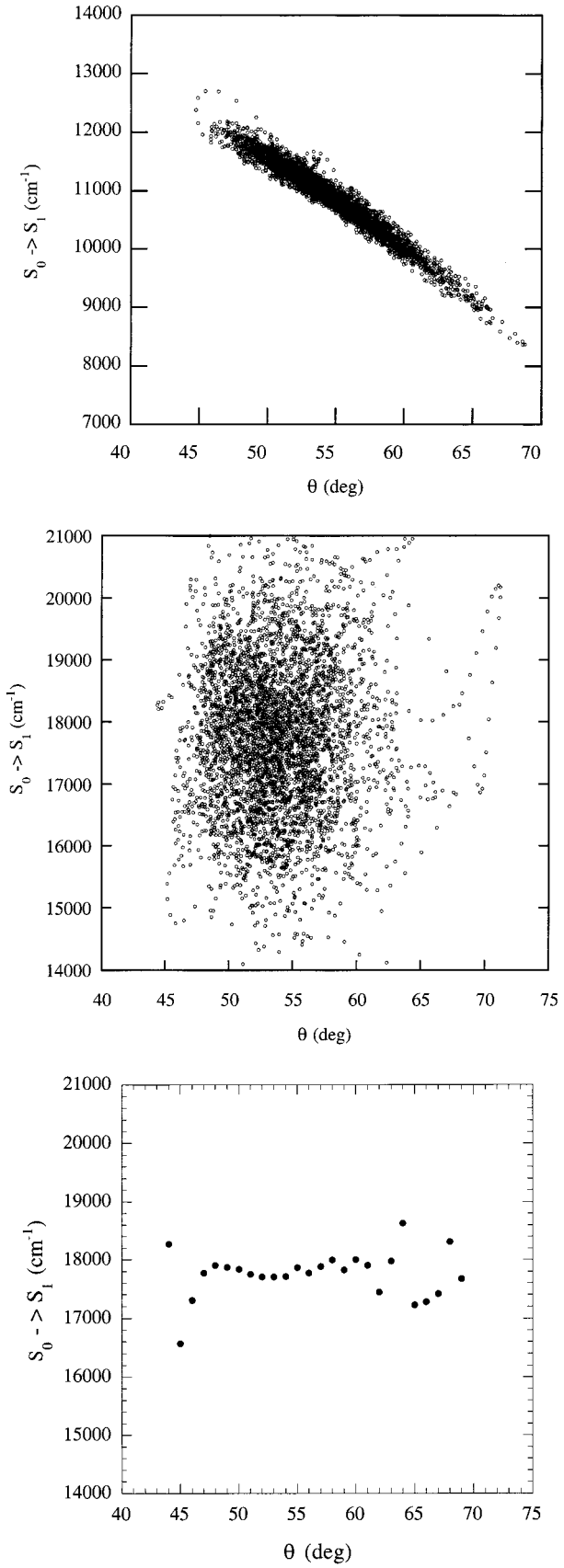

Figure 6. Correlation diagram for the S_0 to S_1 transition energy versus the central ring torsion angle θ. (a) Transition energies calculated omitting solvent interactions in eq 8. (b) Transition energies calculated including the solvent interactions in eq 8. (c) Mean values of the transition energies including the solvent interactions in eq 8, from Figure 6(b).

component from that due to solvent by spectral differences between polar and nonpolar solutions[5] is not supported by the present results. In particular, the good agreement between experiment and calculation obtained here for both the absorption maximum and reorganization energy for the solution phase suggests that the classical (low frequency) component of the reorganization energy in the case of acetonitrile and possibly other aprotic polar solvents may come more heavily from the solvent then previously believed. It is particularly interesting to note that resonance Raman data for betaine-30 taken in acetonitrile[52] have been interpreted in terms of a relatively high solvent component of the reorganization energy ($\sim$6000 cm^{-1}), a result that corresponds more closely to the present result than to the cited interpretations of static absorption spectra.[5] Nevertheless, a puzzling difference between these alternative experimental analyses for the high frequency component (not addressed here) remains.

4. Conclusions

The electronic absorption spectrum of betaine-30 in acetonitrile has been simulated and analyzed using a combined MD and electronic structure methodology based on semiempirical PPP electronic Hamiltonian. The minimum energy conformation of the molecule in the gas phase and solution are found to be substantially the same, and this structure agrees well with previous theoretical studies using alternative quantum chemical approximations where comparison is possible. The simplified model reproduces rather well the solvatochromic shift in the absorption maximum, as well as the absolute position, width, and intensity of the lowest energy S_0 to S_1 transition.

Given this basis for confidence in the validity of the model, a calculation of the absorption spectrum without inclusion of the solvent influence has revealed the dramatic effect of solvent orientational polarization on the ground and excited state wave functions and the corresponding transition energies. While the gas phase ground state S_0 dipole moment agrees well with the experimental estimate[2] in relatively nonpolar solvent, a large enhancement (by $\sim$9 D) is found in acetonitrile solution, paralleling corresponding, but somewhat smaller, increases previously reported for a continuum solvent model.[49] The solvent reorganization energy associated with excitation to the S_1 excited state that can be inferred from a fit to the solution absorption spectrum gives a value in good agreement with that inferred from analysis of the experimental spectrum.[5] However, while the fluctuations in the torsion of the central dihedral ring angle of the betaine-30 in acetonitrile are found to be strongly correlated with fluctuations in the transition energy in the gas phase, this correlation is shown to be lost in acetonitrile solution. In this solution, the absorption width is determined solely by the fluctuations in the solvent field and is remarkably independent of the internal torsional coordinates of the betaine-30. Given the good agreement obtained with the solution phase experimental fit, the result suggests that the classical reorganization energy cannot be separated into a solvent contribution and a solvent independent solute intramolecular vibrational component. This conclusion is contrary to assumptions made in some previous theoretical studies[9] as well as in experimental studies[5] of this solution.

The good agreement between the model calculations and experiment obtained here indicates that the model is also a useful one for studying the back electron transfer dynamics of the S_1 state. Such studies will be reported elsewhere.[53]

Acknowledgment. The authors are grateful for support of this research by a grant from the NSF. Partial support for this

work by the Texas Advanced Research Program is also gratefully acknowledged. J.L. has been supported in part by a postdoctoral fellowship from the Natural Sciences and Engineering Research Council of Canada and by an NSF/CISE Postdoctoral Grant (ASC-9704682). We also thank Mark Maroncelli for stimulating discussions.

Supporting Information Available: Appendix developing the dynamical algorithm for adiabatic dynamics with intramolecular constraints. The material is available free of charge via the Internet at http://pubs.acs.org.

References and Notes

(1) Hantzsch, A. *Ber. Dtsch. Chem. Ges.* **1922**, *55*, 953.
(2) Reichardt, C. *Solvents and Solvent Effects in Organic Chemistry*; VCH: Weinheim, New York, 1988.
(3) Reichardt, C. *Angew. Chem., Int. Ed. Engl.* **1979**, *18*, 98.
(4) Kjaer, A. M.; Ulstrup, J. *J. Am. Chem. Soc.* **1987**, *109*, 1934.
(5) Walker, G. C.; Åkesson, E.; Johnson, A. E.; Levinger, N. E.; Barbara, P. F. *J. Phys. Chem.* **1992**, *96*, 3728.
(6) Dogonadze, R. R.; Itskovitch, E. M.; Kuznetsov, A. M.; Vorotyntsev, M. A. *J. Phys. Chem.* **1975**, *79*, 2827.
(7) Dogonadze, R. R.; Kuznetsov, A. M.; Vorotyntsev, M. A.; Zaqaraia, M. G. *J. Electroanal. Chem.* **1977**, *75*, 315.
(8) Isklovitch, E. M.; Ulstrup, J.; Vorotyntsev, M. A. In *The Chemical Physics of Solvation. Part B. Spectroscopy of Solvation*; Dogonadze, R. R., Kálmán, E., Kornyshev, A. A., Ulstrp, J., Eds.; Elsevier: Amsterdam, 1986; Vol. 38; p 223.
(9) Matyushov, D. M.; Schmid, R.; Ladanyi, B. M. *J. Phys. Chem B* **1997**, *101*, 1035.
(10) Mente, S. R.; Maroncelli, M. *J. Phys. Chem. B* **1999**, *103*, 7704.
(11) Luzhkov, V.; Warshel, A. *J. Am. Chem. Soc.* **1991**, *113*, 4491.
(12) Car, R.; Parrinello, M. *J. Phys. Chem.* **1984**, *98*, 10083.
(13) Remler, D. K.; Madden, P. A. *Mol. Phys.* **1990**, *70*, 921.
(14) Levinger, N. E.; Johnson, A. E.; Walker, G. C.; Barbara, P. F. *Chem. Phys. Lett.* **1992**, *196*, 159.
(15) Pariser, R.; Parr, R. G. *J. Chem. Phys.* **1953**, *21*, 466.
(16) Pariser, R.; Parr, R. G. *J. Chem. Phys.* **1953**, *21*, 767.
(17) Pople, J. A. *Trans. Faraday Soc.* **1953**, *49*, 1375.
(18) Murrell, J. N.; Harget, A. J. *Semiempirical Self-Consistent Molecular-Orbital Theory of Molecules*; Wiley-Interscience: London, 1972.
(19) Warshel, A.; Karplus, M. *J. Am. Chem. Soc.* **1972**, *94*, 5612.
(20) Warshel, A.; Lappicirella, A. *J. Am. Chem. Soc.* **1981**, *103*, 4664.
(21) Field, M. J.; Bash, P. A.; Karplus, M. *J. Comput. Chem.* **1990**, *11*, 700.
(22) Szabo, A.; Ostlund, N. S. *Modern Quantum Chemistry*; McGraw-Hill: New York, 1989.
(23) Bailey, M. L. *Theor. Chim. Acta* **1969**, *13*, 56.
(24) Nishimoto, K.; Forster, L. S. *Theor. Chim. Acta* **1966**, *4*, 155.
(25) Hinze, J.; Jaffe, H. H. *J. Am. Chem. Soc.* **1962**, *84*, 540.
(26) Linderberg, J. *Chem. Phys. Lett.* **1967**, *1*, 39.
(27) Atkins, P. W. *Molecular Quantum Mechanics*; Oxford University Press: Oxford, 1983.
(28) Chung, A. L. H.; Dewar, M. J. S. *J. Chem. Phys.* **1963**, *42*, 756.
(29) Bartell, L. S. *J. Chem. Phys.* **1960**, *32*, 827.
(30) Fischer-Hjalmers, I. *Tetrahedron* **1963**, *19*, 1805.
(31) Edwards, D. M. F.; Madden, P. A.; McDonald, I. R. *Mol. Phys.* **1984**, *51*, 1141.
(32) Allen, M. P.; Tildesley, D. J. *Computer Simulation of Liquids*; Oxford University Press: Oxford, 1987.
(33) Grozema, F. C.; van Duijnen, P. T. *J. Phys. Chem. A* **1998**, *102*, 7984.
(34) Perng, B.-C.; Newton, M. D.; Raineri, F. O.; Friedman, H. L. *J. Chem. Phys.* **1996**, *104*, 7177.
(35) Gao, J. J. *J. Am. Chem. Soc.* **1994**, *116*, 9324.
(36) Thompson, M. A. *J. Phys. Chem.* **1996**, *100*, 14492.
(37) Bader, J. S.; Berne, B. J. *J. Chem. Phys.* **1996**, *104*, 1293.
(38) Pulay, P. In *Ab initio Methods in Quantum Chemistry-II*; Lawley, K. P., Ed.; John Wiley & Sons Ltd.: New York, 1987; Vol. 69.
(39) Förner, W. *Solid State Comm.* **1987**, *63*, 941.
(40) Nosé, S. *Mol. Phys.* **1984**, *52*, 255.
(41) Nosé, S. *J. Chem. Phys.* **1984**, *81*, 511.
(42) Hoover, W. G. *Phys. Rev. A* **1985**, *31*, 1695.
(43) Steinhauser, O. *Mol. Phys.* **1982**, *45*, 335.
(44) Andersen, H. C. *J. Comput. Phys.* **1983**, *52*, 24.
(45) Ryckaert, J.-P.; Ciccotti, G.; Berendson, H. J. C. *J. Comput. Phys.* **1977**, *23*, 327.
(46) Ciccotti, G.; Ferrario, M.; Ryckaert, J.-P. *Mol. Phys.* **1982**, *47*, 1253.
(47) Hurley, M. M.; Hammes-Schiffer, S. *J. Phys. Chem.* **1997**, in press.
(48) Martyna, G. J.; Klein, M. L.; Tuckerman, M. *J. Chem. Phys.* **1992**, *97*, 2635.
(49) Alencastro, R. B. d.; Neto, J. D. D. M.; Zerner, M. C. *Int. J. Quantum Chem. Quantum Chem. Symp.* **1994**, *28*, 361.
(50) Bartkowiak, W.; Lipinski, J. *J. Phys. Chem. A* **1998**, *102*, 5236.
(51) Steinfeld, J. I. *Molecules and Radiation: An Introduction to Modern Molecular Spectroscopy*, 2nd ed.; MIT Press: Cambridge, MA, 1985.
(52) Zong, Y.; McHale, J. L. *J. Chem. Phys.* **1997**, *106*, 4963.
(53) Lobaugh, J.; Rossky, P. J. *J. Phys. Chem.* **1999**, in press.
(54) Jorgensen, W. L.; Briggs, J. M.; Contreras, M. L. *J. Phys. Chem.* **1990**, *94*, 1683.
(55) Jorgensen, W. L.; Severance, D. L. *J. Am. Chem. Soc.* **1990**, *112*, 4768.